3904 *Biochemistry* **2009,** *48,* 3904–3914
DOI:10.1021/bi900189e

BIOCHEMISTRY
including biophysical chemistry & molecular biology
Article

Interrogating the Molecular Details of the Peroxiredoxin Activity of the *Escherichia coli* Bacterioferritin Comigratory Protein Using High-Resolution Mass Spectrometry†

David J. Clarke,*,‡ C. Logan Mackay,‡ Dominic J. Campopiano,‡ Pat Langridge-Smith,‡ and Alan R. Brown§,∥

‡*School of Chemistry, University of Edinburgh, West Mains Road, Edinburgh EH9 3JJ, U.K.,* §*Department of Medical Microbiology, Centre for Infectious Diseases, University of Edinburgh, 49 Little France Crescent, Edinburgh, EH16 4SB, U.K.* ∥*Current address: School of Biosciences, University of Exeter, Stocker Road, Exeter EX4 4QD, U.K*

Received February 5, 2009. Revised Manuscript Received March 19, 2009

ABSTRACT: Bacterioferritin comigratory protein (BCP) is a bacterial thioredoxin-dependent thiol peroxidase that reduces a variety of peroxide substrates. Using high-resolution Fourier transform ion cyclotron resonance mass spectrometry coupled with top-down fragmentation techniques, we have analyzed the mechanistic details of hydrogen peroxide reduction by *E. coli* BCP. We show here that catalysis occurs via an atypical two-cysteine peroxiredoxin pathway. A transient sulfenic acid is initially formed on Cys-45, before resolution by the formation of an intramolecular disulfide bond between Cys-45 and Cys-50. This oxidized BCP intermediate is shown to be a substrate for reduction by thioredoxin, completing the catalytic cycle. Although we invoke Cys-50 in the catalytic cycle of *Escherichia coli* bacterioferritin comigratory protein (BCP), a previous study had shown that this residue was not absolutely required for peroxiredoxin activity. In order to explain these apparently conflicting phenomena, we analyzed the reaction of a C50S BCP mutant with peroxide. We show that this mutant BCP enzyme adopts a different and novel mechanistic pathway. The C50S BCP mutant reacts with peroxide to form a sulfenic acid on Cys-45, in the same manner as wild-type BCP. However, the nascent intermediate is then resolved by reaction with Cys-45 from a second BCP molecule, resulting in a dimeric intermediate containing an intermolecular disulfide bond. We further show that this novel resolving complex is a substrate for reduction by thioredoxin. The importance of our results in furthering the understanding of catalysis within BCP family is discussed.

Reactive oxygen species (ROS) arise from incomplete reduction of molecular oxygen and are potentially damaging to all cellular macromolecules including DNA, proteins, and membrane lipids (*1*, *2*). Organisms defend themselves against ROS damage through the catalytic action of enzymes such as peroxidases, superoxide dismutases, and catalases which, acting alone or in sequence, reduce ROS to water or alcohols.

Among the antioxidant proteins, the most recently discovered are the peroxiredoxins (Prxs; EC 1.11.1.15), enzymes which reduce hydroperoxides using electrons derived from NADPH (*3*−*6*). These non-heme peroxidases utilize a highly reactive cysteine residue to decompose peroxides and are found in all branches of life. Prxs have been shown to reduce a wide variety of substrates, including hydrogen peroxide, peroxinitrite, and organic peroxides (*7*−*11*). Furthermore, they are expressed at high intracellular levels: in *E. coli* they are among the ten most abundant cellular proteins, and in eukaryotic erythrocytes they are the second or third most abundant protein (*12*, *13*).

Prxs have been classified into two categories, the 1-Cys and 2-Cys Prxs, based on the number of cysteines required for catalysis (Scheme 1). The 2-Cys peroxidases have been further delineated into typical and atypical 2-Cys peroxidases (*6*, *14*). All Prxs appear to have a common first step, which involves a conserved cysteine thiolate attacking the peroxide substrate, resulting in the formation of a sulfenic acid intermediate on the cysteine (Cys-SOH) and a RO^- leaving group (which is presumably subsequently protonated). This active cysteine has been termed the peroxidatic cysteine (Cys-S_PH). The resolution of the sulfenic acid intermediate occurs via a different pathway in the three classes of Prxs. The typical 2-Cys Prxs are obligate dimers, which contain two identical active sites. In this class, during resolution of the sulfenic acid intermediate a second cysteine residue, known as the resolving cysteine (Cys-S_RH), from one subunit attacks the sulfenic acid intermediate (Cys-S_POH) of the other

*Corresponding author. Tel: +44-131-651-3034. Fax: +44-131-650-4743. E-mail: dave.clarke@ed.ac.uk.

†This work was supported by the RASOR consortium, EPSRC, BBSRC, CF Trust, Big Lottery, and the University of Edinburgh.

 Published on Web 3/19/2009 © 2009 American Chemical Society

Scheme 1

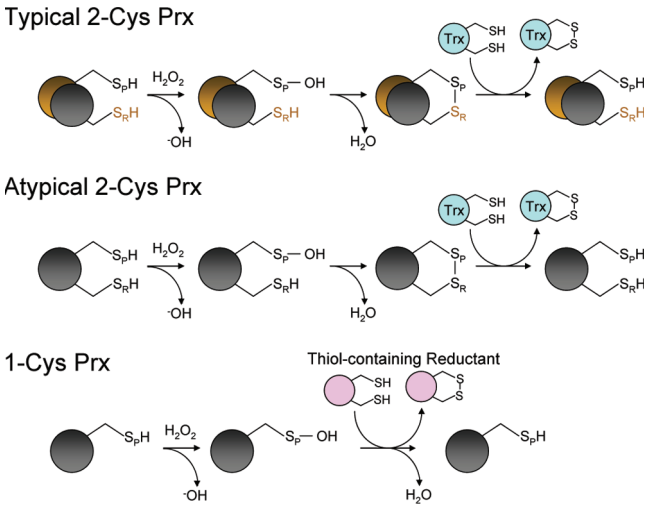

subunit, resulting in an intermolecular disulfide bridge between the two subunits. The catalytic cycle is completed by the reduction of this disulfide bond by a cell-specific oxidoreductase. The atypical 2-Cys Prxs share the same basic mechanism as typical 2-Cys Prxs, with the exception that the atypical 2-Cys enzymes are functionally monomeric and the resolving cysteine is, in most cases, located on the same polypeptide chain as the peroxidatic cysteine. Thus, resolution of the intermediate sulfenic acid (Cys-S_POH) results in an intramolecular disulfide bond. All known atypical 2-Cys peroxidases appear to use thioredoxin to reduce this disulfide and complete the catalytic cycle (*6*). In contrast, 1-Cys Prxs do not contain a resolving cysteine. Little is known about the resolution of the sulfenic acid in this class of Prxs, although various small molecule electron donors have been implicated in the role, including glutathione, lipoic acid, cyclophilin, and ascorbate (*15*−*18*). In recent years, the lines between the different classes of Prx have become somewhat blurred, and it is apparent that these classifications are not absolute. Moreover, it has been demonstrated that 2-Cys Prxs can be converted into 1-Cys Prxs by mutation of the resolving cysteine, suggesting some intrinsic mechanistic adaptability within the superfamily (*19*−*21*).

Bacterioferritin comigratory protein (BCP)[1] is an *E. coli* protein of mass 18 kDa, which displays the same electrophoretic mobility as bacterioferritin (*22*). The primary structure of *E. coli* BCP has similarities with Prx proteins, and it has been demonstrated that *E. coli* BCP has thioredoxin-dependent peroxidase activity (*23*). Homologues of BCP are ubiquitous in the prokaryotic kingdom, and examples have also been found in higher eukaryotes; the plant homologue of BCP is peroxiredoxin Q (PrxQ), which is expressed only in leaves and is localized in the chloroplasts and the guard cells of stomata (*24*). Recent studies in *Helicobacter pylori* have linked BCP with bacterial pathogenicity, and BCP was shown to contribute significantly to the ability of the bacteria to colonize the host's stomach (*25*, *26*).

In this study we use high-resolution mass spectrometry (FT-ICR-MS) to study the peroxiredoxin reaction catalyzed by *E. coli* BCP. The ultrahigh resolving power and mass accuracy of FT-ICR-MS allow determination of the accurate mass of intact proteins, which permits the detection of protein modifications with high confidence. Furthermore, the use of top-down tandem MS fragmentation methodologies enables location of these modifications on the polypeptide chain, without the need for lengthy proteolytic digestion, chromatographic separation, and peptide analysis (*27*−*29*). To date, this methodology has predominantly been applied to the study of protein post-translational modifications (PTMs) (*30*), although, more recently, these techniques have also been used for the interrogation of covalent enzyme intermediates (*31*−*37*). We find that incubation of recombinant *E. coli* BCP with H_2O_2 leads to the oxidation of the cysteine thiol of Cys-45 to sulfenic acid. We subsequently observed conversion of this sulfenic acid to an intramolecular disulfide bond through reaction with Cys-50 and found that this intermediate was reduced by thioredoxin back to the dithiol enzyme. We used similar techniques to study the intermediates in a C50S BCP mutant. This enzyme also oxidized to a sulfenic acid but was then resolved by the Cys-45 thiol from another monomer to generate a dimer linked by an intermolecular S−S bond. These results lead us to reevaluate the classification of *E. coli* BCP within the peroxiredoxin superfamily and highlight the utility of FT-ICR MS and top-down fragmentation in enzymology.

EXPERIMENTAL PROCEDURES

Reagents and Chemicals. Molecular biology grade dithiothreitol (DTT) was purchased from Invitrogen (Carlsbad, CA). All LC solvents and ammonium acetate were purchased from Fischer Chemicals (Zurich, Switzerland) and were of HPLC or LC-MS grade. *N*-Ethylmaleimide (NEM) and tris(2-carboxyethyl)phosphine hydrochloride (TCEP) were purchased from Pierce (Rockford, IL). Hydrogen peroxide, iodoacetamide (IAM), and 7-chloro-4-nitrobenz-2-oxa-1,3-diazole (NBD-Cl) were purchased from the Sigma-Aldrich Chemical Co. (St. Louis, MO).

Recombinant Expression of E. coli BCP and C50S BCP. The DNA sequence encoding *E. coli* BCP was amplified from *E. coli* K-12 genomic DNA by PCR and cloned into pET-28a (Novagen, Madison, WI). The protein was expressed with a 20-residue N-terminal tag containing a six-histidine motif to allow isolation by immobilized metal affinity chromatography. The C50S BCP mutant was prepared using QuikChange mutagenesis (Stratagene). Expression plasmids were transformed into the *E. coli* strain BL21(DE3) for protein expression. Typically, cells were grown to an OD_{600} of 0.6 at 37 °C, and protein expression was induced with 0.25 mM isopropyl β-D-thiogalactoside for 3 h at 37 °C. Both wild-type and C50S BCP were expressed with N-terminal

[1]Abbreviations: BCP, bacterioferritin comigratory protein; Prx, peroxiredoxin; ROS, reactive oxygen species; Cys-S_PH, peroxidatic cysteine; Cys-S_RH, resolving cysteine; PAGE, polyacrylamide gel electrophoresis; MES, 2-(*N*-morpholino)ethanesulfonic acid; OD_{600}, optical density at 600 nm; DTT, 1,4-dithiothreitol; NEM, *N*-ethylmaleimide; TCEP, tris(2-carboxyethyl)phosphine hydrochloride; IAM, iodoacetamide; NBD-Cl, 7-chloro-4-nitrobenz-2-oxa-1,3-diazole; FT-ICR-MS, Fourier transform ion cyclotron resonance mass spectrometry; MS, mass spectrometry; ECD, electron capture dissociation; CID, collision-induced dissociation; Da, daltons; ppm, parts per million.

His_6 tags. Cells were harvested by centrifugation, lysed by sonication, and purified using a HisTrap affinity column on an AKTA FPLC system (GE Healthcare; Supporting Information Figure S1). Eluted protein was stored at 4 °C in 100 mM ammonium acetate (pH 7.2) and used within 7 days of purification. Protein concentrations were measured using the BCA assay (Pierce, Rockford, IL), and both proteins were determined to be >90% pure by protein PAGE.

Preparation of Reduced Thioredoxin. Thioredoxin (*E. coli*) was purchased from the Sigma Chemical Co. and resuspended in 100 mM ammonium acetate (pH 7.2) before reduction with 2 mM TCEP. Excess TCEP was removed by buffer exchange using a PD-Miditrap desalting column (GE Healthcare), and the sample was eluted in 50 mM ammonium acetate, pH 5.5. Disulfide bond reduction was verified by FT-ICR-MS, and the reduced protein was stored at 4 °C. Protein concentration was measured using the BCA assay (Pierce, Rockford, IL).

H_2O_2 Oxidation. Typically, BCP and C50S BCP were at a concentration of 50 μM in ammonium acetate (100 mM, pH 7.2) before reaction with H_2O_2. Oxidation was allowed to proceed for various times before the addition of 4-fold H_2O:MeOH:HCOOH (50:48:2 v/v/v) quenched the reaction.

Sample Reduction and Alkylation. All experiments were performed in ammonium acetate (100 mM, pH 7.2). Reduction was performed by treatment with 1 mM TCEP or 10 mM DTT. For NEM alkylation, proteins were treated with 5 mM *N*-ethylmaleimide and incubated at 22 °C for 5−30 min. Iodoacetamide alkylation was performed by incubation with 10 mM iodoacetamide at 22 °C for 60 min in the dark.

Modification of C50S BCP with 7-Chloro-4-nitrobenz-2-oxa-1,3-diazole (NBD-Cl). C50S BCP (50 μM) in ammonium acetate (100 mM, pH 7.2) was pretreated with 1 mM NBD-Cl before immediate addition of 100 μM H_2O_2. The reaction was allowed to proceed for 1 h in the dark. H_2O:MeOH:HCOOH (50:48:2 v/v/v) was then added to quench the reaction and leave the sample at a final concentration of 10 μM for FT-ICR-MS analysis. A reaction without H_2O_2 was used as a control.

Reaction of Oxidized BCP Species with Reduced Thioredoxin. Oxidized wild-type and C50S BCP species were produced by treatment with varying concentrations of hydrogen peroxide and purified by a PD-Miditrap desalting column (GE Healthcare). The samples (10 μM) were then treated with 20 μM reduced thioredoxin and incubated at room temperature for 5 min. If alkylation was subsequently performed, the sample was then treated with 10 mM iodoacetamide for 1 h in the dark. The reaction was quenched with 2-fold H_2O:MeOH:HCOOH (50:48:2 v/v/v) and analyzed by FT-ICR-MS.

Protein PAGE. Protein PAGE was performed using the Nu-PAGE system (Invitrogen). For all analyzes 4−12% Bis-Tris gels were used, partnered with MES running buffer. Before analysis samples were treated with 4× LDS sample buffer containing 4% β-mercaptoethanol (v/v) and heated to 80 °C for 5 min. For analysis of C50S BCP dimerization nonreducing Nu-PAGE analysis was employed, and β-mercaptoethanol was omitted from the sample buffer. C50S BCP (50 μM) was treated with varying concentrations of H_2O_2 and incubated at room temperature for 2 min before being alkylated with 10 mM NEM. Alkyation was monitored by MS, and once alkylation was complete, the samples were treated with 4× LDS sample buffer and heated to 80 °C for 5 min. All gels were stained with Gelcode Blue stain reagent (Pierce).

FT-ICR Mass Spectrometry. Before FT-ICR-MS analysis each sample was quenched with 4-fold H_2O:MeOH:HCOOH (50:48:2 v/v/v), resulting in a protein concentration of approximately 10 μM. Mass spectrometry data were acquired on an Apex Ultra Qh-FT-ICR mass spectrometer equipped with a 12 T superconducting magnet and an electrospray ion source (Bruker Daltonics, Billerica, MA). Nano-ESI was performed using a TriVersa Nanomate (Advion BioSciences, Ithaca, NY) running in infusion mode. Desolvated ions were transmitted to a 6 cm Infinity cell penning trap. Trapped ions were excited (frequency chirp 48−500 kHz at 100 steps of 25 μs) and detected between m/z 600 and 3000 for 0.5 s to yield broad-band 512K or 1 Mword time-domain data. Each spectrum was the sum of 32 mass analyses. The mass spectra were externally calibrated using ES tuning mix (Agilent) and analyzed using DataAnalysis software (Bruker Daltonics).

Top-Down FT-ICR Tandem Mass Spectrometry. Top-down fragmentation was performed on the 12 T Qh-FT-ICR. First, a specific ion species was isolated with the instrument's mass resolving quadrupole, and MS/MS was performed using collision-induced dissociation (CID) or electron capture dissociation (ECD) (*38*−*40*). For CID, the collision voltage was typically set between 20 and 35 V. For ECD, 1.8 A was applied to the dispenser cathode filament (Heatwave Technologies), 20 V to the lens, and a pulse of 4−9 ms was employed. Fragmentation data were the sum of 250−750 scans, and data analyses were performed using DataAnalysis (Bruker Daltonics). The SNAP algorithm was used for automated peak picking, and the resulting top-down fragment mass lists were searched against the primary sequence of BCP using Prosight-PTM software (*41*, *42*). Mass error tolerances were set for all Prosight searches at 10 ppm.

Isotopic Modeling. Isotope distributions of specific charge states were predicted using IsotopePattern software (Bruker Daltonics) from theoretical empirical formulas. These were overlaid upon the recorded experimental data as scatter plots, with the theoretical apex of each isotope peak designated by a circle.

RESULTS

E. coli BCP Acts as an Atypical 2-Cys Peroxidase. Although *E. coli* BCP has been shown to possess Prx activity *in vitro*, little is known about its mechanism of action. *E. coli* BCP contains three cysteine residues (Cys-45, Cys-50, and Cys-99); however, only one, Cys-45, is absolutely conserved throughout the BCP cluster (Supporting Information Figure S5). By analysis of a C45S BCP mutant, Jeong and co-workers have shown that this residue is absolutely required for activity, and it is thought to be the peroxidatic cysteine (*23*). In contrast, mutation of Cys-99 in BCP had no effect on enzymatic activity. Of interest, it was found that although mutation

of the Cys-50 residue reduced the activity of the enzyme, the protein still retained ~60% Prx activity compared with wild type. These results were taken to suggest that BCP acts via a 1-Cys pathway, where only the peroxidatic Cys-45 is utilized during catalytic turnover. In order to test this hypothesis, we have employed high-resolution mass spectrometry to directly monitor the oxidation state of BCP before and after treatment with hydrogen peroxide. Surprisingly, upon addition of 200 μM H_2O_2 to BCP we observed a decrease in mass consistent with the loss of two hydrogen atoms (Δmass −2 Da), suggesting the formation of a disulfide bond (Figure 1A−C). The formation of the disulfide was confirmed by treatment with the cysteine thiol alkylating reagent *N*-ethylmaleimide (NEM), which resulted in the addition of only one alkyl group (Δmass +125.047 Da, Figure 1D). This monoalkylated species was then reduced with DTT to break the disulfide bond and subjected to top-down fragmentation using either CID or ECD (CID fragmentation was performed on the $[M + 15H]^{15+}$ charge state at *m*/*z* 1321.18, and ECD fragmentation was performed on the $[M + 18H]^{18+}$ charge state at *m*/*z* 1101.16). Fragment mass lists were searched against the primary structure of BCP using Prosight-PTM software, and both techniques produced fragments which allowed the assignment of the NEM moiety to Cys-99 and the disulfide bond to Cys-45−Cys-50 (Figure 2). The formation of this disulfide between Cys-45−Cys-50 was observed using a wide range of H_2O_2 concentration, from 50 μM (1 mol equiv) to 50 mM (1000 mol equiv). Disulfide bond formation was complete within 5 s, the shortest time we could reproducibly perform and quench the reaction.

Localization of the Peroxidatic Cysteine to Cys-45 and Capture of a Sulfenic Acid Intermediate. The above result

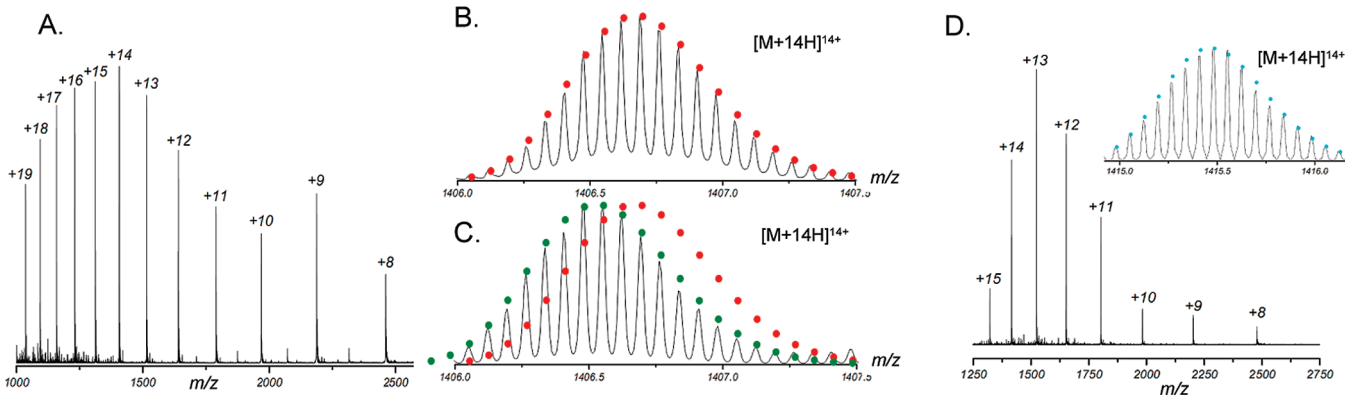

FIGURE 1: Accurate mass measurement of BCP before and after addition of hydrogen peroxide. (A) Typical ESI mass spectrum of *E. coli* BCP acquired in positive ion mode under denaturing conditions. Each charge state is annotated. (B) *E. coli* BCP before addition of H_2O_2. The isotope distribution of the $[M + 14H]^{14+}$ charge state is consistent with the theoretical isotope distribution of BCP containing three reduced cysteine residues (red circles; empirical formula $[C_{873}H_{1348}N_{244}O_{263}S_7]^{14+}$). (C) *E. coli* BCP after addition of 200 μM H_2O_2. The isotope distribution reveals a mass shift of −2 Da, which is consistent with the formation of one disulfide bond (green circles; empirical formula $[C_{873}H_{1346}N_{244}O_{263}S_7]^{14+}$). (D) The disulfide bond was confirmed by treatment with the alkylating reagent NEM. Alkylation resulted in the addition of a single NEM moiety, $[C_6O_2NH_7]$, +125.047 Da. (D, insert) The recorded isotope distribution is consistent with the theoretical isotope distribution of BCP containing one disulfide bond and one NEM-modified cysteine (light blue circles; empirical formula $[C_{879}H_{1353}N_{245}O_{265}S_7]^{14+}$).

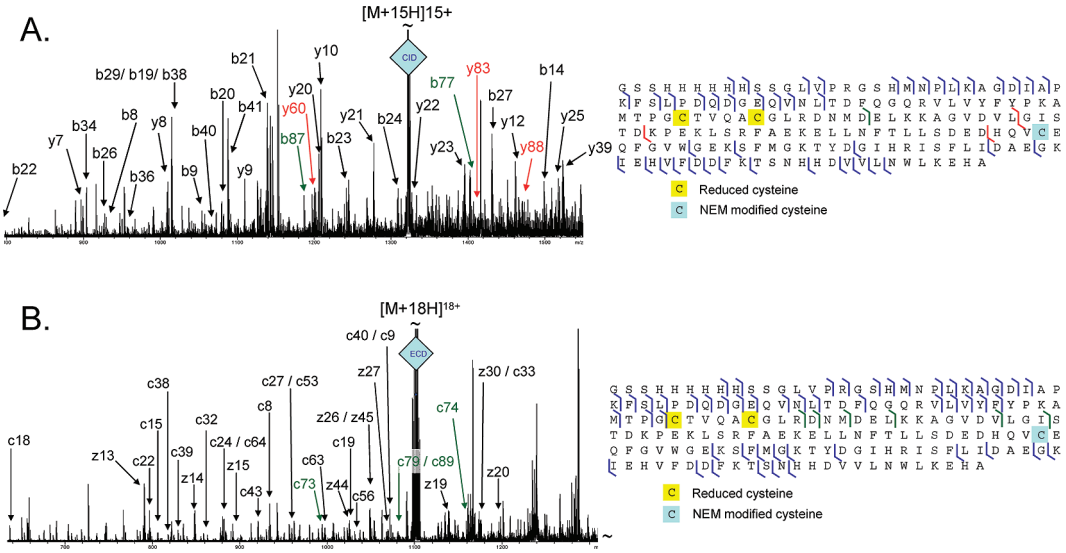

FIGURE 2: Top-down fragmentation of oxidized BCP reveals that the disulfide formed upon addition of peroxide is located between Cys-45 and Cys-50. BCP was treated with 200 μM H_2O_2, which results in the formation of a disulfide bond. The oxidized protein was then treated with the alkylating reagent NEM in order to alkylate the free cysteine. Finally, the disulfide was reduced by addition of the reducing agent DTT. (A) Top-down CID fragmentation of the $[M + 15H]^{15+}$ ion resulted in the 25 *b* ions and 21 *y* ions. (B) Top-down ECD fragmentation of the $[M + 18H]^{18+}$ ion was complementary to the CID data and resulted in the 41 *c* ions and 16 *z* ions. Using both methods 11 ions could be used to assign Cys-99 as the NEM-modified cysteine (*b* and *c* ions labeled in green, *y* ions labeled in red).

led us to hypothesize that *E. coli* BCP uses an atypical 2-Cys peroxiredoxin mechanism, with Cys-45 acting as the Cys-S_PH and Cys-50 as the Cys-S_RH. Interestingly, there is indirect evidence that the plant homologue of BCP from *Sedum lineare*, PrxQ, may act via an atypical 2-Cys pathway (*24*). To verify our hypothesis, we attempted to capture a sulfenic acid intermediate on the peroxidatic cysteine of *E. coli* BCP using the thiol and sulfenic acid labeling reagent NBD-Cl (*43*, *44*).

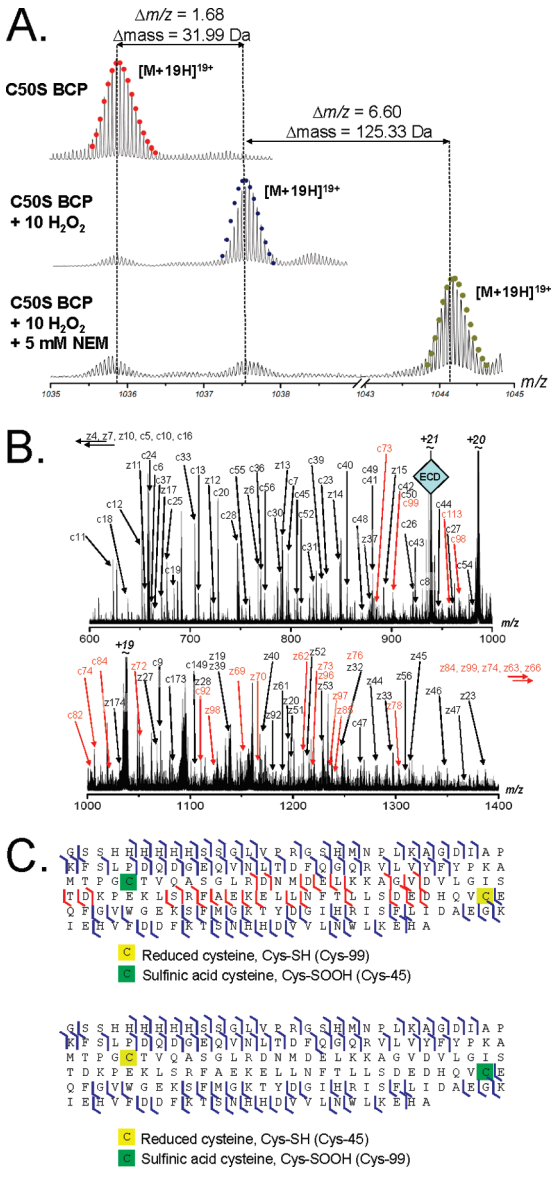

FIGURE 3: The C50S BCP mutant is susceptible to hyperoxidation of the peroxidatic cysteine to a sulfinic acid. (A) The C50S BCP mutant was purified by FPLC with two reduced cysteine residues (red circles; empirical formula $[C_{873}H_{1353}N_{244}O_{264}S_6]^{19+}$). Upon incubation with 10 mol equiv of H_2O_2, a mass increase of 31.9865 Da was observed, consistent with the addition of two oxygen atoms (blue circles; empirical formula $[C_{873}H_{1353}N_{244}O_{266}S_6]^{19+}$). Treatment of the oxidized C50S mutant with NEM resulted in the addition of a single NEM moiety (theoretical isotope distribution, gold circles; empirical formula $[C_{879}H_{1360}N_{245}O_{268}S_6]^{19+}$). (B) Top-down ECD fragmentation of the $[M + 21H]^{21+}$ charge state of H_2O_2-oxidized C50S BCP produced 51 *c* ions and 53 *z* ions. Cleavages which allowed assignment of the sulfinic acid to Cys-45 are highlighted in red. (C) Prosight-PTM output file (cleavage map) demonstrating that 28 fragment ions support the placement of the sulfinic acid to Cys-45 (top), while no fragment ions support the placement of the sulfinic acid to Cys-99 (bottom).

Unfortunately, we were unable to detect the modification on the wild-type protein, presumably because the transient sulfenic acid is quickly resolved by Cys-S_RH forming the stable disulfide bond.

In order to capture and locate the sulfenic acid intermediate, we produced a recombinant C50S BCP mutant, with the hypothetical Cys-S_RH replaced with a serine. Upon exposure of this mutant enzyme to 500 μM H_2O_2 we did not observe disulfide bond formation; instead, the mass of the protein increased by 32 Da, consistent with covalent modification with two oxygen atoms (Figure 3A). This was attributed to hyperoxidation of the peroxidatic cysteine to the sulfinic acid form (Cys-S_POOH), a reported modification of peroxidatic cysteines, and a stable redox state of cysteine (*45*−*47*). This was confirmed by reacting the H_2O_2-treated C50S mutant with NEM, which resulted in the addition of only a single NEM moiety. This established that only one cysteine thiol was available for alkylation and that the H_2O_2-induced two-oxygen atom modification took place on a single cysteine residue and was indeed sulfinic acid formation. This overoxidation proved advantageous; the hyperoxidized species, with its peroxidatic cysteine residue distinguishable by a mass shift of 32 Da, was stable to ESI conditions, allowing us to perform top-down fragmentation to locate the peroxidatic cysteine sulfinic acid. The $[M + 21H]^{21+}$ charge state was isolated and subjected to MS/MS using ECD, and the resulting MS/MS spectra are shown in Figure 3B. Fragment mass lists were searched against the primary structure of BCP using Prosight-PTM software, and 28 fragment ions were detected which allowed us to assign the sulfinic acid modification to Cys-45. No fragments were observed which corresponded to the alternate cysteine modifications (Figure 3C). These results are in agreement with previous reports which suggest that Cys-45 is the peroxidatic center of *E. coli* BCP (*23*).

In order to prevent overoxidation and to capture the enzyme intermediate sulfenic acid, the C50S mutant was treated with NBD-Cl. This electrophilic labeling reagent reacts specifically with both Cys-SH and Cys-S-OH to produce Cys-S-NBD adducts and Cys-S(O)-NBD adducts, respectively (*44*). Crucially, upon reaction with NBD-Cl, the oxygen atom from a sulfenic acid is retained within the product, producing a mass label which is stable to the ESI-MS process. Using this labeling strategy and high-resolution mass analysis, we were able to capture the sulfenic acid intermediate as its stable Cys-S(O)-NBD conjugate (Figure 4). When C50S BCP was oxidized with H_2O_2 in the presence of NBD-Cl, a species with an isotope distribution matching C50S BCP containing one Cys-S-NBD conjugate and one Cys-S(O)-NBD conjugate ($[C_{885}H_{1352}N_{250}O_{271}S_6]^{16+}$) was clearly observed. Due to the unstable nature of the sulfenic acid intermediate, which had a propensity to overoxidize to the sulfinic acid or to form an intermolecular disulfide bond (see below), it was necessary to pretreat the protein with NBD-Cl immediately before oxidation with peroxide. This resulted in the presence of a C50S BCP species containing two Cys-S-NBD conjugates in the resulting reaction mixture, presumably formed by the peroxidatic cysteine reacting with NDB-Cl before the addition of peroxide.

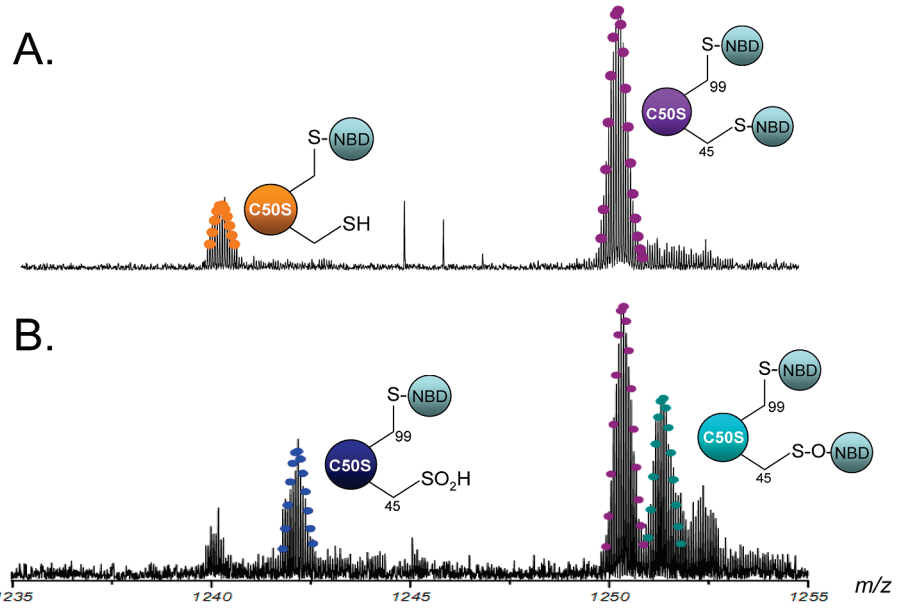

FIGURE 4: FT-ICR mass spectra showing the NBD-modified products of the reduced and H_2O_2-oxidized C50S BCP and analysis of the $[M + 16H]^{16+}$ charge state. 50 μM C50S BCP was reacted with a 100-fold excess of NBD-Cl with or without prior oxidation by 1 mol equiv of H_2O_2. (A) Analysis of the reaction products of reduced C50S BCP and NBD-Cl revealed one major product, consistent with the modification of both cysteines to Cys-S-NBD (purple circles; empirical formula $[C_{885}H_{1352}N_{250}O_{270}S_6]^{16+}$). A small amount of single NBD-modified protein was also present (orange circles; empirical formula $[C_{879}H_{1351}N_{247}O_{267}S_6]^{16+}$). (B) NBD-Cl treatment of C50S BCP oxidized with H_2O_2 produced a second species with an isotope distribution consistent with C50S BCP containing one Cys-S-NBD conjugate and one Cys-S(O)-NBD conjugate (cyan circles; empirical formula $[C_{885}H_{1352}N_{250}O_{271}S_6]^{16+}$). A third species was observed which corresponds to C50S BCP with one Cys-SOOH and one Cys-S-NBD (blue circles; empirical formula $[C_{879}H_{1351}N_{247}O_{269}S_6]^{16+}$).

However, if the enzyme was oxidized with peroxide before addition of the labeling reagent, the major reaction product was oxidation at Cys-45, and consequently little trapped sulfenic acid was observed. Interestingly, we also observed a minor species corresponding to C50S BCP with one Cys-SOOH and one Cys-S-NBD. It is evident that the C50S BCP mutant is prone to hyperoxidation even upon treatment with stoichiometric quantities of peroxide and in the presence of NBD-Cl.

Oxidized BCP Is Reduced by Thioredoxin. In the reductive step of the 2-Cys Prx catalytic cycle, thioredoxin (Trx) is believed to be responsible for the reduction of oxidized Prxs to return the enzyme to its fully reduced state. Indeed, initial kinetic analysis has demonstrated that *E. coli* BCP can utilize Trx as a reductant *in vitro*. However, it is unclear what BCP oxidation state is the natural substrate for Trx. In order to verify that oxidized BCP, containing a disulfide bond between Cys-45 and Cys-50, is a substrate for Trx, we analyzed the redox exchange reaction by FT-ICR MS. Oxidized BCP was prepared by treating reduced BCP with 10 equivalents of H_2O_2 and was monitored by observing the characteristic 2 Da mass decrease. The third cysteine thiol was subsequently alkylated with NEM to produce a species containing a disulfide bond between Cys-45 and Cys-50 and Cys-99-S-NEM (as observed in Figure 1D). This species was then incubated with 2 equivalents of reduced thioredoxin. Any resulting cysteine thiols were then alkylated with iodoacetamide, and the reaction mixture was analyzed by FT-ICR-MS. Upon mass spectrometric analysis of the mixture we observed a mass shift in the BCP species equivalent to carbamidomethyl modification of two cysteine residues, indicating the reduction of the disulfide bond between Cys-45 and Cys-50 upon addition of Trx, thus demonstrating that Trx efficiently reduces the oxidized BCP enzyme intermediate (Supporting Information Figure S2).

These combined results suggest that the *E. coli* BCP mechanism occurs via an atypical 2-Cys Prx pathway. If this is indeed the case, then we would expect that both Cys-45 and Cys-50 would be essential for Prx activity. However, it has been previously reported that although Cys-45 is strictly required for catalysis, removal of Cys-50 does not abolish activity (*23*). Furthermore, analysis of the BCP family shows that Cys-50 is not strictly conserved across all BCP homologues. These observations imply that the BCP can complete the Prx catalytic cycle via a different "resolving complex" without the need for Cys-50.

Analysis of the Catalytic Mechanism of the C50S BCP Mutant. Treatment of BCP C50S with Excess Peroxide Results in Overoxidation of Cys-45 to a Sulfinic Acid. In order to elucidate this alternate catalytic mechanism, we used FT-ICR-MS to monitor the oxidation of the C50S BCP mutant by varying amounts of H_2O_2 (Figure 5). As we have already noted, the C50S BCP mutant is prone to hyperoxidation of its Cys-S_PH to sulfinic acid. This overoxidation is prevalent after incubation of C50S BCP with greater than 5 mol equivalents of H_2O_2 (Figure 5B, blue circles). Indeed, with a large excess of H_2O_2 (>250 mol equivalents), we also observed the appearance of a significant amount of sulfonic acid modification (Figure 5B, orange circles). This hyperoxidation is in stark contrast to wild-type BCP, which produces a stable Cys-45−Cys-50 disulfide bond even in the presence of 250 mol equivalents of H_2O_2 (see Figure 5A, green circles). Surprisingly, moderate peroxide treatment (<10-fold H_2O_2) of the C50S mutant produces a second species with Δmass -2 Da, which indicates a loss of two hydrogen atoms (Figure 5B, green circles). We believe this minor species

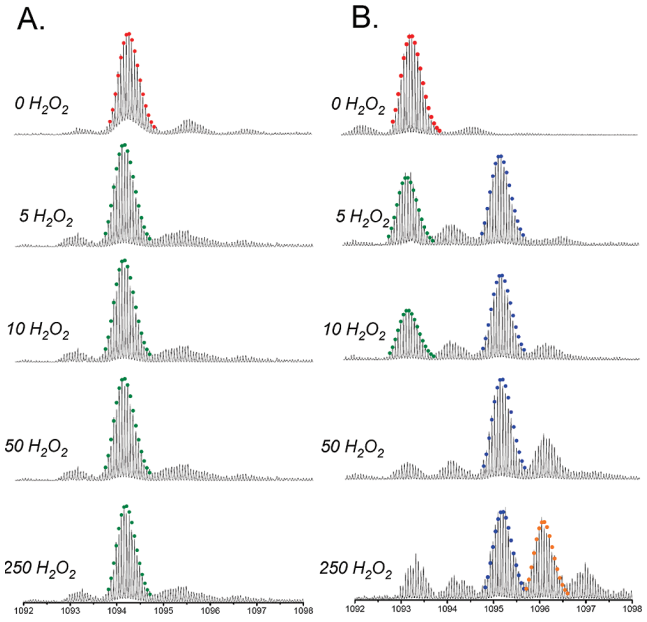

FIGURE 5: Susceptibility of wild-type BCP and C50S BCP to hyperoxidation by excess peroxide treatment. Aliquots of BCP or C50S BCP (50 μM) were incubated with varying amounts of H_2O_2 for 10 min before MS analysis. Here the $[M + 18H]^{18+}$ charge state is shown. (A) Addition of peroxide to wild-type BCP results in formation of the Cys-45−Cys-50 disulfide bond via an atypical 2-Cys peroxiredoxin pathway (theoretical isotope distribution for BCP containing one disulfide bond, green circles; empirical formula $[C_{873}H_{1350}N_{244}O_{263}S_7]^{18+}$). The Cys-45−Cys-50 disulfide bond was resistant to overoxidation, even at 250 molar excess of H_2O_2. (B) Addition of peroxide to C50S BCP results in the formation of a stable hyperoxidized sulfinic acid localized on Cys-45 (blue circles; empirical formula $[C_{873}H_{1352}N_{244}O_{266}S_6]^{18+}$). With 50 mol equiv or more a significant amount of sulfonic acid modification was also observed (theoretical orange circles; empirical formula $[C_{873}H_{1352}N_{244}O_{267}S_6]^{18+}$). With < 10-fold peroxide a second species was observed with a Δmass of −2 Da (green circles; empirical formula $[C_{873}H_{1350}N_{244}O_{263}S_7]^{18+}$).

is due to the formation of an unstable disulfide between Cys-45 and Cys-99.

Treatment of C50S BCP with Stoichiometric Quantities of Peroxide Produces an Intermolecular Disulfide-Linked Dimer. It is clear that the C50S mutant is prone to overoxidation to form the inactive sulfinic acid derivative in the presence of excess peroxide, a property which we assume is responsible for the reduced activity of this mutant. In order to minimize the hyperoxidation of the Cys-S_PH, the oxidation of C50S BCP by stoichiometric quantities of peroxide was studied by mass spectrometry. Within 30 s of peroxide treatment, two species were observed in the mass spectrum. The first species had a mass consistent with a BCP C50S monomer with a loss of 2 Da (Figure 6A, green circles) and is attributed to the formation of a disulfide between Cys-45 and Cys-99, while the second species had a mass consistent with a C50S BCP dimer (Figure 6A, claret circles). Isotope modeling of the $[M + 29H]^{29+}$ and $[M + 30H]^{30+}$ charge states of this dimeric species reveals that the mass is consistent with that calculated for a C50S dimer containing one intermolecular disulfide bond and two cysteine thiols (Figure 6B, claret circles). This assignment was confirmed by reaction of the C50S BCP dimer with NEM, which resulted in an increase in mass of +250 Da, consistent with the addition of two NEM moieties and signifying the presence of only two free thiol groups within the dimer (Supporting Information Figure S3A). Furthermore, reaction of the C50S BCP dimer with the chemical reducing agents TCEP or DTT resulted in the appearance of a single species, with isotope distributions consistent with C50S BCP containing two reduced cysteines (Cys-45-SH and Cys-99-SH), confirming that dimerization of the C50S mutant is indeed mediated by an intermolecular disulfide bond (Supporting Information Figure S3B). We were also able to observe this dimerization by protein PAGE using nonreducing conditions, where a species of mass ~40 kDa is observed after treatment of C50S BCP with peroxide (Figure 6C). For PAGE analysis, 50 μM C50S BCP was oxidized with varying concentrations of peroxide for 2 min. In order to block any free cysteine thiols, thus restricting thiol−disulfide exchange, alkylation with 10 mM NEM was performed prior to gel analysis.

Efficient dimerization of BCP C50S was observed upon oxidation with 0.5 mol equiv of peroxide (Figure 6C, lane 2). As the titer of peroxide increases, more monomeric C50S BCP is observed (Figure 6C, lanes 3−5). Presumably, this is due to overoxidation of the sulfenic acid to the sulfinic acid effectively competing with intermolecular disulfide bond formation. Interestingly, protein PAGE analysis suggests that the dimeric form of C50S BCP is far more prominent than the monomeric form after mild peroxide treatment. In contrast, the MS data have consistently less intense peaks for the dimeric species in relation to the monomeric species (Figure 6A, bottom). We believe this is due to the ionization efficiency of each species during the ESI process. The heavier dimeric species is less efficiently ionized and detected relative to the lighter monomeric species. Consequently, the relative intensities of each ion series cannot be directly compared in order to deduce their relative quantities. Indeed, we believe that protein PAGE analysis represents a more accurate depiction of relative abundance and the dimeric form of the oxidized protein predominates.

Derivitization and Top-Down Analysis of the Oxidized C50S BCP Dimer Reveal the Intermolecular Disulfide Is Formed between Cys-45 and Cys-45′. In order to deduce which cysteine residues are involved in the intermolecular disulfide bond, we again utilized top-down tandem MS fragmentation. The intermolecular disulfide bond was formed by addition of 1 mol equiv of H_2O_2 to 50 μM C50S BCP; the two free thiol cysteines were then alkylated by incubation with NEM, resulting in a C50S dimer containing one intermolecular disulfide bond and two Cys-S-NEM derivatives. This species was subsequently chemically reduced with DTT to produce two monomers of the same mass, both containing one reduced Cys-SH and one Cys-S-NEM (see Supporting Information Figure S4). Presumably, one monomer contained Cys-45-S_PH and Cys-99-S-NEM, which originated from the molecule containing the Cys-45-S_POH intermediate, while the position of the NEM on the "resolving" monomer would be dependent on which Cys residue was involved in the intermolecular disulfide bond. This derivatized species was analyzed by nano-ESI-FT-ICR-MS, and five charge states (+16 to +21) were systematically isolated and subjected to MS/MS using ECD. The resulting fragments were then grouped and analyzed using Prosight-PTM (Figure 7). Of the 113 assigned fragment ions, 27 were

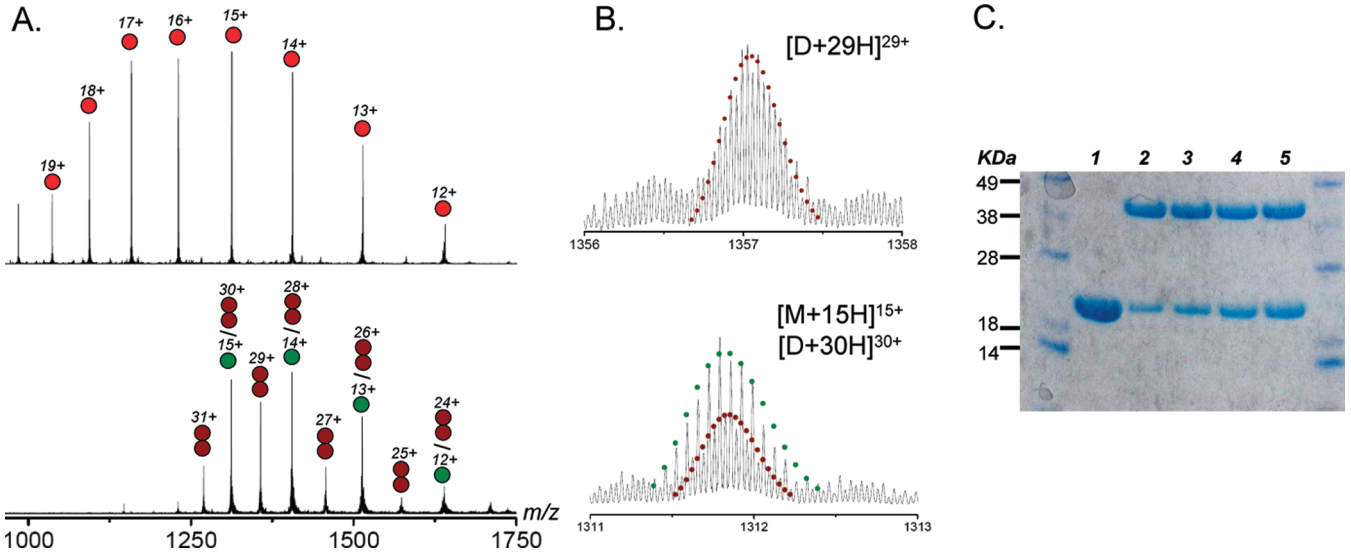

FIGURE 6: Mild peroxide oxidation of C50S BCP leads to formation of an intermolecular disulfide bond. (A) FT-ICR-MS analysis of C50S BCP before (top) and after (bottom) 100 μM H_2O_2 treatment. The charge-state distribution of the reduced C50S BCP protein is highlighted with the red circles. Upon addition of H_2O_2 two species are observed: an oxidized monomer containing an intramolecular disulfide between Cys-45 and Cys-99 (charge-state distribution labeled with green circles) and an oxidized dimer containing an intramolecular disulfide bond (charge-state distribution labeled with claret circles). (B) Analysis of the isotope distribution of the H_2O_2-treated C50S BCP mutant. (Top) The peak at m/z 1357 has an isotope distribution consistent with the $[D + 29H]^{29+}$ charge state of C50S BCP containing one intermolecular disulfide bond (claret circles; empirical formula $[C_{1746}H_{2695}N_{488}O_{528}S_{12}]^{29+}$). (Bottom) The peak at m/z 1405 contains two isotope patterns: one consistent with the $[M + 15H]^{15+}$ charge state of monomeric C50S BCP containing an intramolecular disulfide (green circles; empirical formula $[C_{873}H_{1348}N_{244}O_{264}S_6]^{15+}$) and the other consistent with the $[D + 30H]^{30+}$ charge state of C50S BCP containing one intermolecular disulfide bond (claret circles; empirical formula $[C_{1746}H_{2696}N_{488}O_{528}S_{12}]^{30+}$). (C) Nonreducing PAGE analysis: lane 1, 50 μM C50S BCP before addition of H_2O_2; lanes 2–5, C50S BCP after addition of 25, 50, 200, and 1000 μM H_2O_2 and alkylation with 10 mM NEM.

diagnostic of the Cys-99-S-NEM modification; no fragments were observed which would indicate that the Cys-45-S-NEM modification was present (Figure 7B). These results strongly suggest that the intermolecular disulfide is formed between Cys-45 and Cys-45′.

The Oxidized C50S BCP Dimer Is Reduced by Thioredoxin. For complete peroxiredoxin catalytic turnover the oxidized resolving complex must be efficiently reduced to the dithiol form. As we have demonstrated above, for the wild-type enzyme this can be achieved by the oxidoreductase thioredoxin. Enzyme assay experiments suggest that the C50S mutant can also utilize thioredoxin in this fashion (*23*). In order to determine if thioredoxin can also efficiently reduce the Cys-45−Cys-45′ disulfide bond in the C50S BCP dimer, we studied the redox exchange reaction by FT-ICR-MS. C50S BCP was oxidized by treatment of the protein with 1 molar equivalents of H_2O_2 for 10 min, and appearance of the dimeric species was verified by MS. This species was then incubated with 2 molar equivalents of reduced thioredoxin for 5 min before FT-ICR-MS analysis. MS analysis showed two species were present (Figure 8). The BCP species displayed a charge-state distribution consistent with a monomeric species, and isotope analysis revealed a distribution consistent with fully reduced C50S BCP (Figure 8B, red dots; empirical formula). These results clearly demonstrate that the intermolecular disulfide bond in the resolving complex of C50S BCP is efficiently reduced by thioredoxin.

DISCUSSION

In this study we have established the mechanistic details of catalysis performed by the peroxiredoxin BCP from *E. coli* and a single-cysteine BCP variant. This has been accomplished using recombinant technology, site-directed mutagenesis, chemical modification, and mass spectrometry. Direct interrogation as to the nature and location of enzyme intermediates has been achieved using FT-ICR mass spectrometry coupled with top-down fragmentation methodologies. This is the first time that a peroxiredoxin reaction mechanism has been delineated using mass spectrometry.

We have demonstrated that the highly conserved Cys-45 within BCP acts as the peroxidatic cysteine and is oxidized to a sulfenic acid intermediate upon treatment with excess peroxide. This catalytic intermediate is subsequently resolved by reaction with Cys-50, forming an internal Cys-45−Cys-50 disulfide bond. We have also demonstrated that the catalytic cycle can be completed by reduction of the Cys-45−Cys-50 disulfide bond by thioredoxin (Scheme 2A). Thus, we provide strong evidence that the mechanism of catalysis of wild-type BCP follows the atypical 2-cysteine peroxiredoxin pathway (*6*). This classification of *E. coli* BCP is contrary to previous reports which suggest that the enzyme acts via a 1-cysteine pathway (*23*, *48*). Our classification is essentially the same as that proposed for the plant homologue of BCP, PrxQ (*24*, *49*).

However, unlike the plant PrxQ, the catalytic activity of *E. coli* BCP is not absolutely reliant on the presence of the resolving cysteine Cys-50. A BCP mutant lacking Cys-50 still displays thioredoxin-dependent peroxidase activity *in vitro* (*23*). By examining the reaction of recombinant C50S BCP with peroxide by FT-ICR-MS, we believe an alternative and distinct reaction pathway is utilized by this mutant. Upon mild peroxide treatment we observed that the C50S mutant quickly formed a stable dimeric species. FT-ICR-MS analysis of this species reveals that dimerization is mediated by an intermolecular disulfide bond

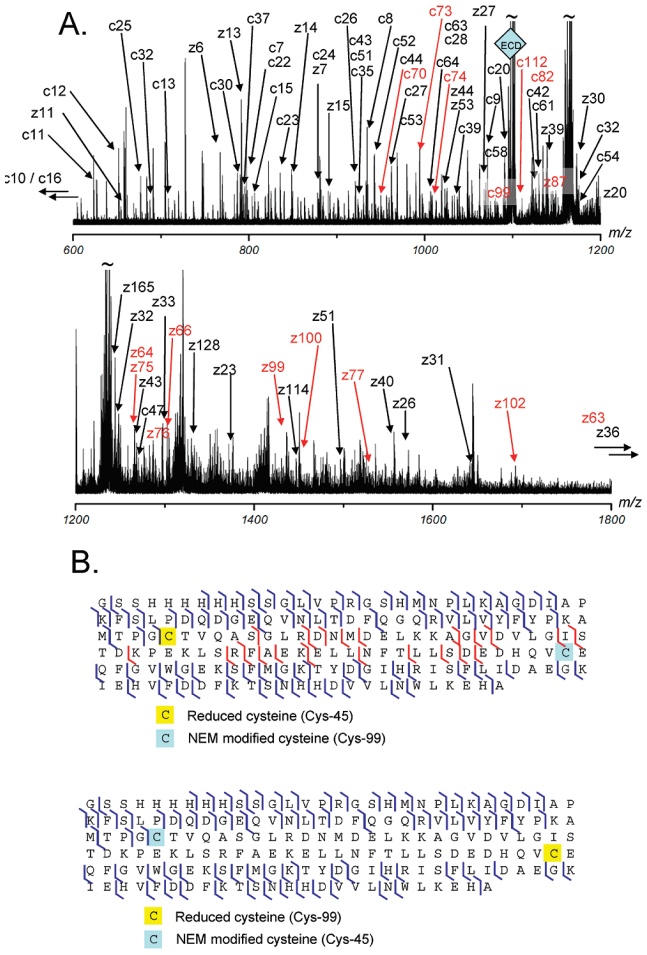

FIGURE 7: Top-down fragmentation of the oxidized C50S BCP dimer. BCP was treated with 50 μM H_2O_2, which results in the formation of an intermolecular disulfide bond. The oxidized dimer was then treated with the alkylating reagent NEM in order to alkylate the free cysteines. Finally, the disulfide was reduced by addition of the reducing agent DTT. (A) Top-down ECD fragmentation of five charge states resulted in a total of 57 assigned *c* ions and 56 assigned *z* ions. Here the ECD spectra of the $[M + 18H]^{18+}$ charge state is shown. (B) Prosite PTM output files (cleavage map) demonstrating that 27 assigned fragments are diagnostic of a NEM-modified Cys-99 residue (top), while no fragments were diagnostic of an NEM-modified Cys-45 residue (bottom).

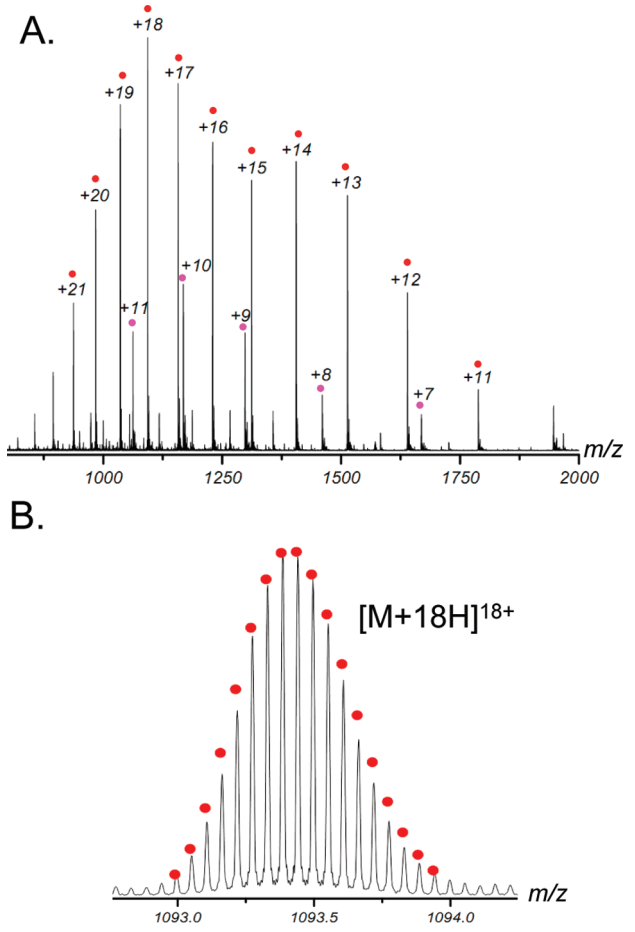

FIGURE 8: FT-ICR-MS analysis demonstrating that thioredoxin can efficiently reduce the Cys-45−Cys-45′ intermolecular disulfide in the C50S BCP dimer. The C50S BCP dimer was formed by treatment of 50 μM C50S BCP with 50 μM H_2O_2. This species was then treated with 2 equiv of reduced thioredoxin for 5 min before the reaction was quenched and analyzed by FT-ICR-MS. (A) MS analysis revealed two major species: the C50S BCP ion series is highlighted with red dots, and the thioredoxin ion series is highlighted with pink dots. (B) The isotope distribution of the C50S BCP species is consistent with the theoretical isotope distribution of fully reduced C50S BCP (red dots; empirical formula $[C_{873}H_{1352}N_{244}O_{263}S_7]^{18+}$).

between the two monomers via residue Cys-45 (forming a Cys-45−Cys-45′ dimer). Our interpretation of this result is that the C50S mutant initially forms a sulfenic acid on Cys-45 by reduction of peroxide. This intermediate is then resolved by the attack on the sulfenic acid by the thiolate form of a second Cys-45, forming the intermolecular disulfide bond. In effect, Cys-45 is initially acting as the peroxidatic cysteine, before Cys-45 from a second monomer acts as a resolving cysteine. We have also demonstrated that this resolving complex is efficiently reduced by thioredoxin, allowing the completion of the catalytic cycle (Scheme 2B). We also show that the C50S mutant is susceptible to hyperoxidation of the peroxidatic cysteine to sulfinic acid. This phenomenon, which occurs under high levels of peroxide substrate, is common in Prx isoforms that lack the conserved resolving cysteine. It is thought to occur because the sulfenic acid intermediate is not efficiently converted to a stable disulfide by reaction with a nearby Cys-S_RH; instead, the sulfenic acid

Scheme 2

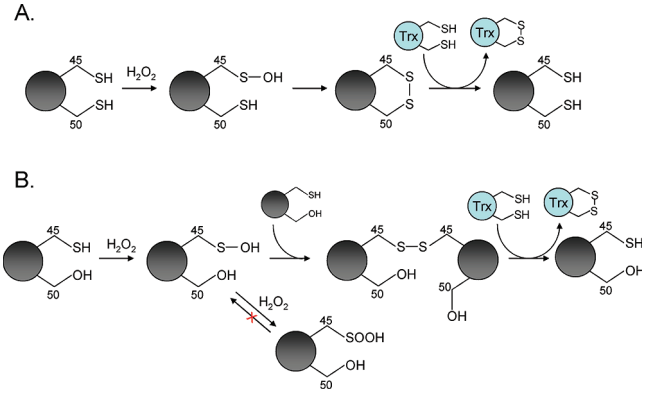

(in its sulfenate anion form) can attack a second peroxide substrate, further oxidizing to the sulfinic acid.

Therefore, it appears that the ability of the C50S mutant to catalyze peroxide reduction is highly sensitive to the level of the peroxide substrate. At low peroxide levels

the sulfenic acid intermediate, Cys-45-SOH, is resolved by Cys-45-S^- from a second molecule forming the Cys-45-S−S-Cys-45′ resolving complex. However, increasing the concentration of peroxide substrate will presumably increase the rate of Cys-45-SOH formation and, therefore, reduce the supply of Cys-45-S^- available to act as the resolving cysteine. Consequently, at higher levels of peroxide the reaction of the sulfenic acid intermediate with a second molecule of peroxide dominates, resulting in hyperoxidation of Cys-45 to sulfinic acid and inactivation of the enzyme. We assume that this irreversible overoxidation pathway is responsible for the observed reduction in activity of the C50S mutant (*23*).

Interestingly, this interconversion of Prx mechanisms upon cysteine deletion has been suggested for other classes of Prxs (*19*−*21*, *50*, *51*). In these examples, removal of the resolving cysteine is assumed to lead to the conversion of a mechanistically classified 2-cysteine Prx to a 1-cysteine Prx; the Cys-S_POH intermediate becomes a direct substrate for a reducing substrate. However, in the example of removing the Cys-S_RH from BCP, outlined above, the mutant enzyme adopts a novel peroxiredoxin mechanistic pathway. This is the first reported example of a peroxiredoxin, albeit an engineered enzyme, which utilizes the same cysteine residue to act as the peroxidatic center and the resolving nucleophile.

It is noteworthy that the presence of the resolving cysteine at position 50 actually represents a minor subset of the bacterial BCP family, being largely confined to gammaproteobacteria, and particularly the *Enterobacteriaceae*. Instead, the majority of BCP homologues from across diverse bacterial genera lack this resolving cysteine (Supporting Information Figure S5). We are currently investigating the nature of catalysis used by the members of the BCP family which lack this residue. We hope to ascertain whether the novel mechanism reported here in the engineered *E. coli* C50S BCP is utilized by the natural BCP homologues in which the resolving cysteine is absent.

ACKNOWLEDGMENT

We wish to thank Prof. Neil Kelleher for the use of Prosight-PTM software.

SUPPORTING INFORMATION AVAILABLE

PAGE analysis of protein purification, thioredoxin reduction assay, and mass spectrometry data showing the derivitization protocol for the C50S BCP dimer. This material is available free of charge via the Internet at http://pubs.acs.org.

REFERENCES

1. Fridovich, I. (1978) The biology of oxygen radicals. *Science 201*, 875–880.
2. Djordjevic, V. B. (2004) Free radicals in cell biology. *Int. Rev. Cytol. 237*, 57–89.
3. Chae, H. Z., Chung, S. J., and Rhee, S. G. (1994) Thioredoxin-dependent peroxide reductase from yeast. *J. Biol. Chem. 269*, 27670–27678.
4. Wood, Z. A., Schroder, E., Robin Harris, J., and Poole, L. B. (2003) Structure, mechanism and regulation of peroxiredoxins. *Trends. Biochem. Sci. 28*, 32–40.
5. Immenschuh, S., and Baumgart-Vogt, E. (2005) Peroxiredoxins, oxidative stress, and cell proliferation. *Antioxid. Redox Signaling 7*, 768–777.
6. Poole, L. B. (2007) The catalytic mechanism of peroxiredoxins. *Subcell. Biochem. 44*, 61–81.
7. Jacobson, F. S., Morgan, R. W., Christman, M. F., and Ames, B. N. (1989) An alkyl hydroperoxide reductase from *Salmonella typhimurium* involved in the defense of DNA against oxidative damage. Purification and properties. *J. Biol. Chem. 264*, 1488–1496.
8. Poole, L. B., and Ellis, H. R. (1996) Flavin-dependent alkyl hydroperoxide reductase from *Salmonella typhimurium*. 1. Purification and enzymatic activities of overexpressed AhpF and AhpC proteins. *Biochemistry 35*, 56–64.
9. Bryk, R., Griffin, P., and Nathan, C. (2000) Peroxynitrite reductase activity of bacterial peroxiredoxins. *Nature (London) 407*, 211–215.
10. Peshenko, I. V., and Shichi, H. (2001) Oxidation of active center cysteine of bovine 1-Cys peroxiredoxin to the cysteine sulfenic acid form by peroxide and peroxynitrite. *Free Radical Biol. Med. 31*, 292–303.
11. Hofmann, B., Hecht, H. J., and Flohe, L. (2002) Peroxiredoxins. *Biol. Chem. 383*, 347–364.
12. Link, A. J., Robison, K., and Church, G. M. (1997) Comparing the predicted and observed properties of proteins encoded in the genome of *Escherichia coli* K-12. *Electrophoresis 18*, 1259–1313.
13. Moore, R. B., Mankad, M. V., Shriver, S. K., Mankad, V. N., and Plishker, G. A. (1991) Reconstitution of Ca(2+)-dependent K^+ transport in erythrocyte membrane vesicles requires a cytoplasmic protein. *J. Biol. Chem. 266*, 18964–18968.
14. Rhee, S. G., Chae, H. Z., and Kim, K. (2005) Peroxiredoxins: a historical overview and speculative preview of novel mechanisms and emerging concepts in cell signaling. *Free Radical Biol. Med. 38*, 1543–1552.
15. Lee, S. P., Hwang, Y. S., Kim, Y. J., Kwon, K. S., Kim, H. J., Kim, K., and Chae, H. Z. (2001) Cyclophilin a binds to peroxiredoxins and activates its peroxidase activity. *J. Biol. Chem. 276*, 29826–29832.
16. Manevich, Y., Feinstein, S. I., and Fisher, A. B. (2004) Activation of the antioxidant enzyme 1-CYS peroxiredoxin requires glutathionylation mediated by heterodimerization with pi GST. *Proc. Natl. Acad. Sci. U.S.A. 101*, 3780–3785.
17. Muller, S. (2004) Redox and antioxidant systems of the malaria parasite Plasmodium falciparum. *Mol. Microbiol. 53*, 1291–1305.
18. Monteiro, G., Horta, B. B., Pimenta, D. C., Augusto, O., and Netto, L. E. (2007) Reduction of 1-Cys peroxiredoxins by ascorbate changes the thiol-specific antioxidant paradigm, revealing another function of vitamin C. *Proc. Natl. Acad. Sci. U.S.A. 104*, 4886–4891.
19. Ellis, H. R., and Poole, L. B. (1997) Roles for the two cysteine residues of AhpC in catalysis of peroxide reduction by alkyl hydroperoxide reductase from *Salmonella typhimurium*. *Biochemistry 36*, 13349–13356.
20. Rouhier, N., Gelhaye, E., and Jacquot, J. P. (2002) Glutaredoxin-dependent peroxiredoxin from poplar: protein-protein interaction and catalytic mechanism. *J. Biol. Chem. 277*, 13609–13614.
21. Trujillo, M., Mauri, P., Benazzi, L., Comini, M., De Palma, A., Flohe, L., Radi, R., Stehr, M., Singh, M., Ursini, F., and Jaeger, T. (2006) The mycobacterial thioredoxin peroxidase can act as a one-cysteine peroxiredoxin. *J. Biol. Chem. 281*, 20555–20566.
22. Neidhardt, F. C., Vaughn, V., Phillips, T. A., and Bloch, P. L. (1983) Gene-protein index of *Escherichia coli* K-12. *Microbiol. Rev. 47*, 231–284.
23. Jeong, W., Cha, M. K., and Kim, I. H. (2000) Thioredoxin-dependent hydroperoxide peroxidase activity of bacterioferritin comigratory protein (BCP) as a new member of the thiol-specific antioxidant protein (TSA)/Alkyl hydroperoxide peroxidase C (AhpC) family. *J. Biol. Chem. 275*, 2924–2930.
24. Kong, W., Shiota, S., Shi, Y., Nakayama, H., and Nakayama, K. (2000) A novel peroxiredoxin of the plant *Sedum lineare* is a homologue of *Escherichia coli* bacterioferritin co-migratory protein (Bcp). *Biochem. J. 351*, 107–114.
25. Wang, G., Hong, Y., Johnson, M. K., and Maier, R. J. (2006) Lipid peroxidation as a source of oxidative damage in *Helicobacter pylori*: protective roles of peroxiredoxins. *Biochim. Biophys. Acta 1760*, 1596–1603.
26. Wang, G., Olczak, A. A., Walton, J. P., and Maier, R. J. (2005) Contribution of the *Helicobacter pylori* thiol peroxidase bacterioferritin comigratory protein to oxidative stress resistance and host colonization. *Infect. Immun. 73*, 378–384.
27. Kelleher, N. L. (2004) Top-down proteomics. *Anal. Chem. 76*, 197A–203A.

28. Siuti, N., and Kelleher, N. L. (2007) Decoding protein modifications using top-down mass spectrometry. *Nat. Methods 4*, 817–821.
29. McLafferty, F. W., Breuker, K., Jin, M., Han, X., Infusini, G., Jiang, H., Kong, X., and Begley, T. P. (2007) Top-down MS, a powerful complement to the high capabilities of proteolysis proteomics. *FEBS J. 274*, 6256–6268.
30. Meng, F., Forbes, A. J., Miller, L. M., and Kelleher, N. L. (2005) Detection and localization of protein modifications by high resolution tandem mass spectrometry. *Mass Spectrom. Rev. 24*, 126–134.
31. Park, J. H., Dorrestein, P. C., Zhai, H., Kinsland, C., McLafferty, F. W., and Begley, T. P. (2003) Biosynthesis of the thiazole moiety of thiamin pyrophosphate (vitamin B1). *Biochemistry 42*, 12430–12438.
32. Dorrestein, P. C., Huili Zhai, H., Taylor, S. V., McLafferty, F. W., and Begley, T. P. (2004) The biosynthesis of the thiazole phosphate moiety of thiamin (vitamin B1): the early steps catalyzed by thiazole synthase. *J. Am. Chem. Soc. 126*, 3091–3096.
33. Dorrestein, P. C., Zhai, H., McLafferty, F. W., and Begley, T. P. (2004) The biosynthesis of the thiazole phosphate moiety of thiamin: the sulfur transfer mediated by the sulfur carrier protein ThiS. *Chem. Biol. 11*, 1373–1381.
34. Xie, L., Miller, L. M., Chatterjee, C., Averin, O., Kelleher, N. L., and van der Donk, W. A. (2004) Lacticin 481: in vitro reconstitution of lantibiotic synthetase activity. *Science 303*, 679–681.
35. McLoughlin, S. M., and Kelleher, N. L. (2004) Kinetic and regiospecific interrogation of covalent intermediates in the nonribosomal peptide synthesis of yersiniabactin. *J. Am. Chem. Soc. 126*, 13265–13275.
36. Kelleher, N. L., and Hicks, L. M. (2005) Contemporary mass spectrometry for the direct detection of enzyme intermediates. *Curr. Opin. Chem. Biol. 9*, 424–430.
37. Godert, A. M., Jin, M., McLafferty, F. W., and Begley, T. P. (2007) Biosynthesis of the thioquinolobactin siderophore: an interesting variation on sulfur transfer. *J. Bacteriol. 189*, 2941–2944.
38. Zubarev, R. A., Kelleher, N. L., and McLafferty, F. W. (1998) Electron capture dissociation of multiply charged protein cations. A nonergodic process. *J. Am. Chem. Soc. 120*, 3265–3266.
39. Zubarev, R. A., Horn, D. M., Fridriksson, E. K., Kelleher, N. L., Kruger, N. A., Lewis, M. A., Carpenter, B. K., and McLafferty, F. W. (2000) Electron capture dissociation for structural characterization of multiply charged protein cations. *Anal. Chem. 72*, 563–573.
40. Cooper, H. J., Hakansson, K., and Marshall, A. G. (2005) The role of electron capture dissociation in biomolecular analysis. *Mass Spectrom. Rev. 24*, 201–222.
41. Leduc, R. D., and Kelleher, N. L. (2007) Using ProSight PTM and related tools for targeted protein identification and characterization with high mass accuracy tandem MS data, *Current Protocols in Bioinformatics*, Chapter 13, Unit 136.
42. LeDuc, R. D., Taylor, G. K., Kim, Y. B., Januszyk, T. E., Bynum, L. H., Sola, J. V., Garavelli, J. S., and Kelleher, N. L. (2004) ProSight PTM: an integrated environment for protein identification and characterization by top-down mass spectrometry. *Nucleic Acids Res. 32*, W340–W345.
43. Poole, L. B., and Ellis, H. R. (2002) Identification of cysteine sulfenic acid in AhpC of alkyl hydroperoxide reductase. *Methods Enzymol. 348*, 122–136.
44. Ellis, H. R., and Poole, L. B. (1997) Novel application of 7-chloro-4-nitrobenzo-2-oxa-1,3-diazole to identify cysteine sulfenic acid in the AhpC component of alkyl hydroperoxide reductase. *Biochemistry 36*, 15013–15018.
45. Yang, K. S., Kang, S. W., Woo, H. A., Hwang, S. C., Chae, H. Z., Kim, K., and Rhee, S. G. (2002) Inactivation of human peroxiredoxin I during catalysis as the result of the oxidation of the catalytic site cysteine to cysteine-sulfinic acid. *J. Biol. Chem. 277*, 38029–38036.
46. Wagner, E., Luche, S., Penna, L., Chevallet, M., Van Dorsselaer, A., Leize-Wagner, E., and Rabilloud, T. (2002) A method for detection of overoxidation of cysteines: peroxiredoxins are oxidized in vivo at the active-site cysteine during oxidative stress. *Biochem. J. 366*, 777–785.
47. Prouzet-Mauleon, V., Monribot-Espagne, C., Boucherie, H., Lagniel, G., Lopez, S., Labarre, J., Garin, J., and Lauquin, G. J. (2002) Identification in *Saccharomyces cerevisiae* of a new stable variant of alkyl hydroperoxide reductase 1 (Ahp1) induced by oxidative stress. *J. Biol. Chem. 277*, 4823–4830.
48. Poole, L. B., Karplus, P. A., and Claiborne, A. (2004) Protein sulfenic acids in redox signaling. *Annu. Rev. Pharmacol. Toxicol. 44*, 325–347.
49. Rouhier, N., Gelhaye, E., Gualberto, J. M., Jordy, M. N., De Fay, E., Hirasawa, M., Duplessis, S., Lemaire, S. D., Frey, P., Martin, F., Manieri, W., Knaff, D. B., and Jacquot, J. P. (2004) Poplar peroxiredoxin Q. A thioredoxin-linked chloroplast antioxidant functional in pathogen defense. *Plant Physiol. 134*, 1027–1038.
50. Montemartini, M., Kalisz, H. M., Hecht, H. J., Steinert, P., and Flohe, L. (1999) Activation of active-site cysteine residues in the peroxiredoxin-type tryparedoxin peroxidase of *Crithidia fasciculata*. *Eur. J. Biochem. 264*, 516–524.
51. Baker, L. M., and Poole, L. B. (2003) Catalytic mechanism of thiol peroxidase from *Escherichia coli*. Sulfenic acid formation and overoxidation of essential CYS61. *J. Biol. Chem. 278*, 9203–9211.